Evidence for aqueous deposition of hematite- and sulfate-rich light-toned layered deposits in Aureum and Iani Chaos, Mars

Timothy D. Glotch[1] and A. Deanne Rogers[2]

[1] Two new gray hematite-rich units have been found in Aureum and Iani Chaos, Mars, using data acquired by the Mars Global Surveyor Thermal Emission Spectrometer. These regions correspond with light-toned sulfate-rich deposits identified by the European Space Agency's OMEGA visible/near-IR spectrometer. Much of the light-toned material in Aureum and Iani Chaos is in the form of a capping unit similar to that seen in Aram Chaos. However, some light-toned material is also seen within the chaotic mounds, indicating that it was present before the formation of the chaotic terrains. The stratigraphy of the units in Iani and Aureum Chaos suggests that the capping and hematite-rich units must have been deposited after the formation of the chaotic terrains in the mid to late Hesperian, up to 1 Gyr after the formation of the light-toned outcrop in Meridiani Planum. The geologic contexts of these and other hematite- and sulfate-rich units in Aram Chaos, Valles Marineris, and Meridiani Planum indicate that they likely formed in similar environments under aqueous conditions. If this is the case, it suggests an active hydrological cycle lasting from the late Noachian to the late Hesperian.

Citation: Glotch, T. D., and A. D. Rogers (2007), Evidence for aqueous deposition of hematite- and sulfate-rich light-toned layered deposits in Aureum and Iani Chaos, Mars, *J. Geophys. Res.*, *112*, E06001, doi:10.1029/2006JE002863.

1. Introduction

[2] The hematite-rich unit in Meridiani Planum was first recognized by the Mars Global Surveyor (MGS) Thermal Emission Spectrometer (TES) instrument [*Christensen et al.*, 2000, 2001]. It represents the uppermost portion of a sequence of layered units [*Hynek et al.*, 2002; *Arvidson et al.*, 2003; *Christensen and Ruff*, 2004; *Edgett*, 2005] and has been investigated in detail by the Mars Exploration Rover (MER) Opportunity [*Squyres et al.*, 2004, 2006; *Squyres and Knoll*, 2005]. The surface of Meridiani Planum consists of a lag of hematite-rich spherules that are eroding out of a light-toned outcrop [*Herkenhoff et al.*, 2004; *Soderblom et al.*, 2004]. This light-toned outcrop is rich in sulfur correlated with magnesium, indicating the presence of magnesium sulfates [*Rieder et al.*, 2004]. In addition, Mössbauer data indicate the presence of the Fe-sulfate jarosite [*Klingelhöfer et al.*, 2004; *Morris et al.*, 2006]. These results were confirmed by the MiniTES instrument, which also detected Ca-sulfates and amorphous silica [*Christensen et al.*, 2004a; *Glotch et al.*, 2006]. Portions of these sandstone outcrops exhibit small-scale trough cross lamination indicative of deposition under aqueous flow [*Squyres et al.*, 2004; *Grotzinger et al.*, 2005].

[3] Meridiani Planum is the site of the largest hematite-rich unit by area on Mars. Smaller hematite-rich units have been described in Aram Chaos [*Christensen et al.*, 2001; *Catling and Moore*, 2003; *Glotch and Christensen*, 2005] and Valles Marineris [*Christensen et al.*, 2001; *Knudson*, 2006]. Like Meridiani Planum, these hematite-rich sites are also host to sulfate-rich deposits [*Gendrin et al.*, 2005]. In this work, we report on (1) two newly discovered hematite-rich units in Aureum and Iani Chaos from analyses of TES data and (2) the distribution of light-toned units in chaotic terrains. These hematite-rich units, like those in Meridiani Planum, Aram Chaos and Valles Marineris, are found in close proximity to light-toned layered deposits. Using data from the European Space Agency's Mars Express Observatoire pour la Mineralogie, l'Eau, les Glaces, et l'Activite (OMEGA) visible/near-IR (VNIR) hyperspectral imager, elevated sulfate concentrations were identified in association with these light-toned units [*Gendrin et al.*, 2005; *Noe Dobrea et al.*, 2006a; *Noe Dobrea*, 2006]. We discuss the relationship between the hematite and light-toned units and evaluate models of formation. Finally, we interpret the geologic settings of Aureum and Iani Chaos and their relation to other hematite-rich regions to determine the most likely scenario for the formation of hematite and sulfate-bearing units on Mars.

2. Methods

[4] Global hematite abundance was mapped using MGS TES data at full spatial resolution from OCKs 1583-7000 (OCK 1 is equivalent to MGS mapping orbit 1683; some science phasing orbit data were used), and by applying the

---

[1] Jet Propulsion Laboratory, California Institute of Technology, Pasadena, California, USA.

[2] Division of Geological and Planetary Sciences, California Institute of Technology, Pasadena, California, USA.
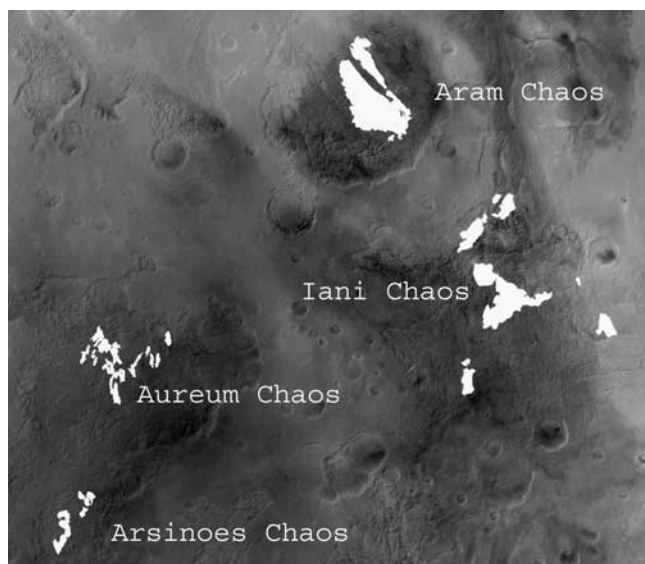
Figure 1. Map of light-toned deposits in chaotic terrains in Margaritifer Terra overlaid on a MOC WA mosaic. The mapped region covers 9°S–4°N latitude and 328–348°E longitude.

hematite spectral index of *Christensen et al.* [2000]. Each TES detector has an instantaneous field of view of ~8.5 mrad, which equates to a spatial resolution of ~3 × 8 km in the final MGS mapping phase altitude. TES data were shifted by 0.271° eastward in longitude to account for the different cartographic systems employed by the MGS and Odyssey spacecraft. Individual TES spectra from regions with high hematite index values were extracted and examined in detail. Factor analysis and target transformation techniques [*Malinowski*, 1991; *Bandfield et al.*, 2000, 2002] were applied to the TES spectra to confirm the presence of crystalline hematite. Finally, linear deconvolution [*Ramsey and Christensen*, 1998] was used to estimate hematite abundance.

[5] *Glotch and Christensen* [2005] mapped several layered units in Aram Chaos, including a light-toned, cliff-forming unit which capped the others (unit Pc). Unit Pc is also distinguished by having a higher nighttime temperature, and therefore thermal inertia, than the surrounding terrain. In this work, we have mapped analogous cap units over a larger region (9°S–4°N, 328–348°E) that includes several other chaotic terrains and the eastern portion of Valles Marineris. Generally, surfaces that shared the following characteristics were classified as light-toned cap units, with an inferred common origin to the Aram Pc unit: (1) higher apparent albedo in visible imagery than surrounding surfaces, (2) higher nighttime temperature than surrounding surfaces, and (3) stratigraphic position above chaotic blocks and other layered units.

[6] Mapping was performed using the JMARS java-based GIS package developed at Arizona State University [*Gorelick et al.*, 2003] (Figure 1). MGS Mars Orbiter Camera (MOC) [*Malin et al.*, 1991, 1992] wide-angle images, a MGS Mars Orbiter Laser Altimeter (MOLA) [*Zuber et al.*, 1992; *Smith et al.*, 2001] 128 ppd shaded relief map, and Mars Odyssey Thermal Emission Imaging

System (THEMIS) [*Christensen et al.*, 2004b] 100 m/pixel infrared mosaics were used as base maps. Higher resolution THEMIS VIS imagery (18 or 36 m/pixel) and MOC narrow angle imagery (~3–5 m/pixel) were used for detailed morphological analysis.

[7] In section 3 we demonstrate that Aram Chaos cap unit exhibits an intrinsic red color apparent in THEMIS VIS images. Thus 36 m/pixel THEMIS VIS color images, where available within the study region, were used to help distinguish the light toned units from the surrounding terrains. Each color image is a false-color stretched combination of THEMIS VIS bands 3, 2, and 1, which are located at 650, 540, and 425 nm respectively. Images have been radiometrically calibrated and projected using the ISIS software package. Details of the calibration of the THEMIS VIS instrument can be found in *McConnochie and Bell* [2003] and *McConnochie et al.* [2006]. Following the method of *Noe Dobrea et al.* [2006b] we created 540 nm band depth images, which provide a good measure of the 540 nm band "kink." The 540 nm "kink" is a feature of the visible spectrum that is diagnostic of the presence of crystalline ferric oxides [*Bell et al.*, 1990, 2004; *Bishop et al.*, 1998; *Morris et al.*, 2000; J. F. Bell III et al., Global color and mineralogic variations on the Martian surface from HST/ WFPC2 multispectral imaging, submitted to *Icarus*, 2006 (hereinafter referred to as Bell et al., submitted manuscript, 2006)] in which the steep red spectral slope abruptly becomes more shallow. To create these images, a "continuum" image was created at the position of the 540 nm band image by linearly interpolating between bands 1 and 3, and the 540 nm band image was divided by this continuum image. The 540 nm band depth (BD) is then defined by:

$$BD = 1 - \left(\frac{Measured\ Band\ 2\ Radiance}{Interpolated\ Band\ 2\ Radiance} \right), \quad (1)$$

where

$$Interpolated\ Band\ 2\ Radiance = 540 \times m + b \quad (2)$$

$$m = \left(\frac{Measured\ Band\ 3\ Radiance - Measured\ Band\ 1\ Radiance}{650 - 425} \right) \quad (3)$$

$$b = Measured\ Band\ 3\ Radiance - (m \times 650) \quad (4)$$

3. Results

[8] Light-toned units with similar thermal and color properties to those in Aram Chaos exist in Iani, Aureum, and Arsinoes Chaos (Figure 1). No light-toned deposits are present on the inter-chaos plains of Margaritifer Terra. Of the mapped deposits, those in Iani and Aureum Chaos exhibit absorptions attributable to sulfates in OMEGA spectra [*Gendrin et al.*, 2005; *Noe Dobrea et al.*, 2006a; *Noe Dobrea*, 2006]. Using the hematite mapping method discussed in section 2, we find that Aureum and Iani Chaos contain gray crystalline hematite units in abundances of up
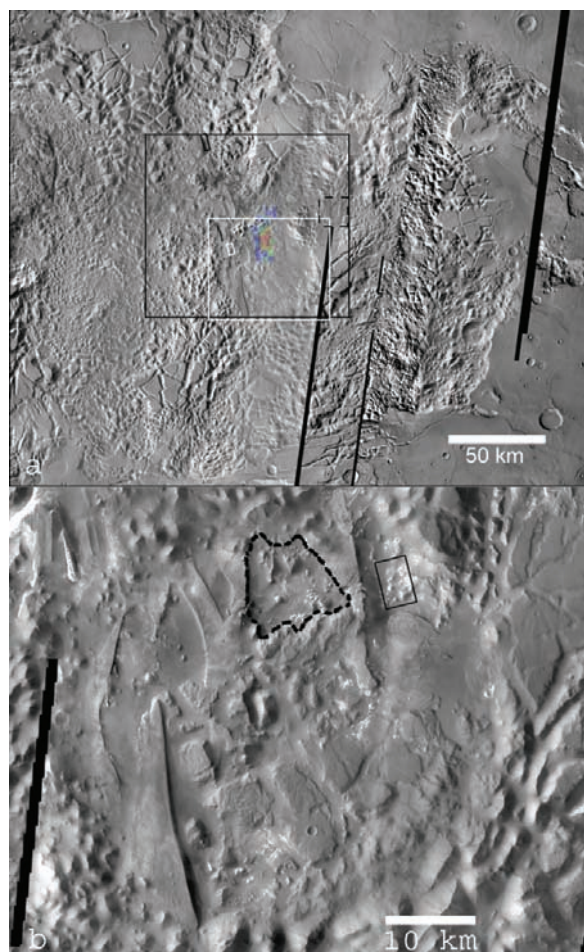
Figure 2. Hematite and light-toned deposits in Aureum Chaos. (a) TES hematite abundance overlaid on THEMIS daytime IR mosaic. Hematite abundance ranges from 5% (blue) to 20% (red). The large white outline shows the location of Figure 2b. The large black outline shows the location of Figure 3a. The small black outline shows the location of Figure 4a. The dashed black outline shows the location of Figure 4c, and the small white outline shows the location of Figure 4d. (b) THEMIS VIS band 3 mosaic consisting of images V14830002, V09002001, V09913001, V11760001, V18811001, V17276001, V08303001, and V13894001, showing the region associated with the highest hematite abundance. The dashed outline is the approximate location of the unit with the highest hematite abundance. The solid black outline indicates the location of Figure 4b. Elevated sulfate concentrations are associated with the light-toned units according to OMEGA data [*Noe Dobrea et al.*, 2006a, *Noe Dobrea*, 2006].

to 20%. A global search was conducted but no other units with greater than 10% hematite contribution to the measured spectrum in two or more contiguous TES pixels were found, including other regions where light-toned deposits have been found such as Arsinoes Chaos (this work), Juventae Chasma [*Catling et al.*, 2006], and Mawrth Vallis, where phyllosilicates have been detected [*Bibring et al.*, 2005; *Poulet et al.*, 2005]. Here, we focus on the relation-

ships between the light-toned and hematite-rich units in Aureum and Iani Chaos and the implications for global hematite mineralization based on our observations.

3.1. Aureum Chaos

[9] Aureum Chaos (Figure 2a) is a 295 km diameter crater centered at 333.0°E, 4.4°S. It is characterized by jumbled, chaotic terrain covering most of the floor. This chaotic terrain is discontinuously overlain in the north-central part of the crater by a smooth, light-toned, cliff-forming unit (Figure 2b) similar to the cap unit (P_c) described in Aram Chaos by *Catling and Moore* [2003] and *Glotch and Christensen* [2005]. In addition, a single gray hematite-rich unit no larger than 75 km^2 in area is present near the center of the crater (Figure 2a). The light-toned unit has an average TES bolometric albedo of ∼0.175. In addition, this unit has a warmer nighttime temperature in THEMIS data (Figure 3a) compared to the surrounding terrain, indicating that it has a higher thermal inertia, which indicates either increased rock abundance or an increased level of cementation compared to the surrounding terrain [*Presley and Christensen*, 1997]. TES thermal inertia [*Jakosky et al.*, 2000; *Mellon et al.*, 2000] of the light-toned unit ranges between ∼295–340 Jm^{-2} s$^{-1/2}$ K^{-1}, compared to a range of ∼260–320 Jm^{-2} s$^{-1/2}$ K^{-1} for the surrounding plains and chaotic terrain.
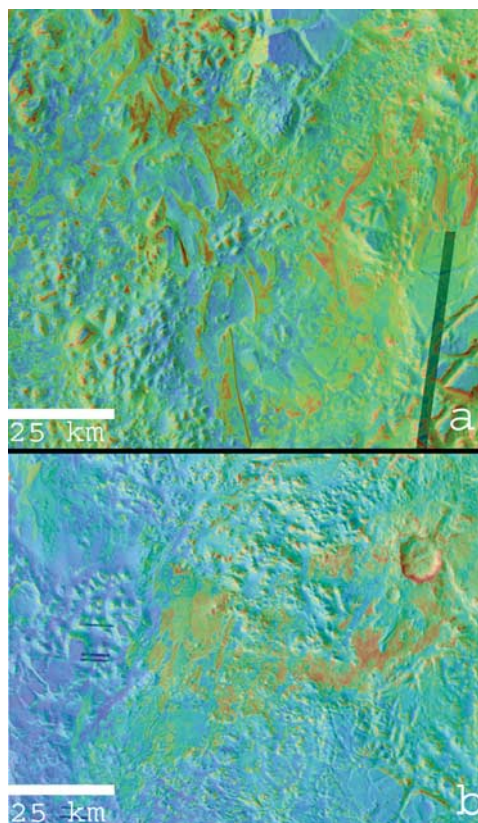
Figure 3. THEMIS nighttime IR radiance mosaic overlaid on THEMIS daytime IR radiance mosaic. Temperatures range from 180 K (blue) to 206 K (red). Other than rocky crater rims and fracture cliffs, the light-toned deposits are the warmest regions in the scene, likely indicating an increase in cementation. (a) Aureum Chaos. (b) Iani Chaos.
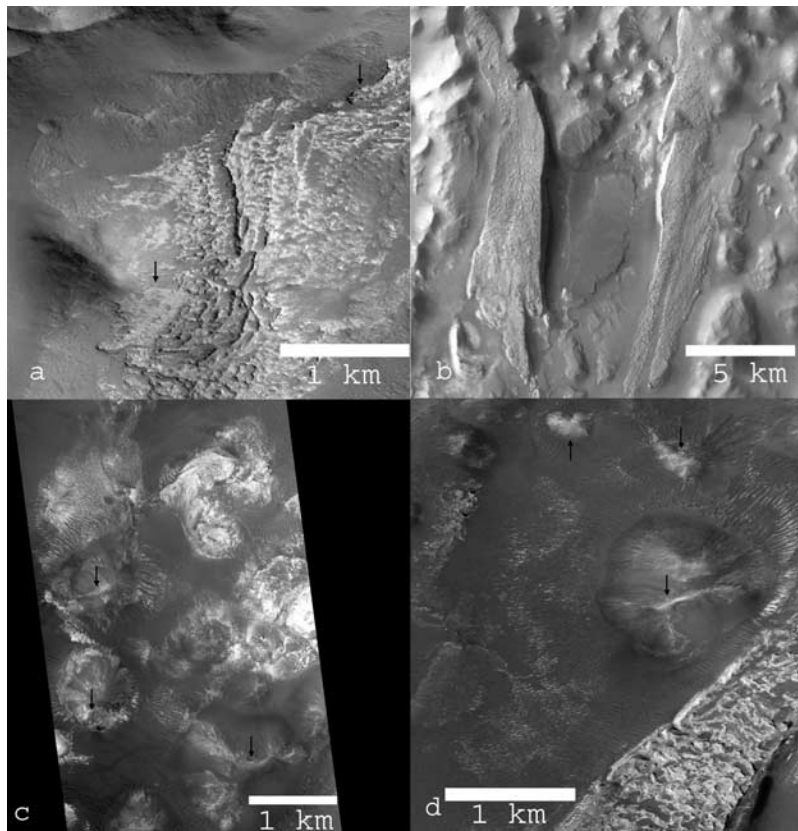
Figure 4. Light-toned deposits in Aureum Chaos are present both above and within chaotic terrain. (a) Portion of MOC NA image R18-01339. Light-toned material on-laps a small mound and a scarp (arrows). (b) THEMIS VIS band 3 mosaic consisting of images V07941001 and V10824001 showing large outcrops of light-toned material conforming to preexisting topography. (c) Portion of MOC NA image E15-00408 showing the presence of light-toned material within and beneath chaotic mounds (arrows). (d) Portion of MOC NA image R10-01646 showing both cliff-forming light-toned caprock and light-toned material present within small chaotic mounds (arrows).

[10] The exact stratigraphy in Aureum Chaos is somewhat difficult to determine due to the ubiquitous presence of dark sand which often obscures contacts between light-toned material and chaotic terrain. However, examples from both MOC NA and THEMIS VIS imagery (Figures 4a and 4b) show the light-toned unit on-lapping chaotic mounds and conforming to preexisting topography. Thus in some areas, it appears that the light-toned unit lies stratigraphically above the chaotic terrain, and was therefore deposited subsequent to chaos formation. While most of the light-toned material in Aureum Chaos is present stratigraphically above the chaotic terrains as a cap unit similar to that seen in Aram Chaos, we note that there are also small exposures of bright material within and below some chaotic mounds (Figure 4c), sometimes in close proximity to the light-toned cap unit (Figure 4d). Although this bright material within and below the mounds does not fit all of the criteria used in regional-scale mapping of light-toned units (section 2), it does exhibit a higher apparent albedo, a higher nighttime temperature, and a redder color than the bulk of the material composing the mounds. However, these bright-toned exposures are too small for large-scale textures to be resolved. Thus, because of the lack of complete information available, we identify these exposures as "tentative light-toned units" and discuss the implications of a potentially common origin to the cap units in section 4.

[11] Figure 2b shows the location of the gray crystalline hematite-rich unit in Aureum Chaos. Hematite abundance within this unit varies from 5–20% by area, which is similar to the range of abundance present in Meridiani Planum and Aram Chaos [*Christensen et al.*, 2000, 2001; *Glotch and Christensen*, 2005]. Hematite spectral features are easily observed in atmospherically uncorrected TES spectra (Figure 5). The hematite-rich unit appears to lie stratigraphically below the light-toned cap unit and above the chaotic mounds, indicating that it, like the cap unit was deposited subsequent to the event leading to the formation of Aureum Chaos.

3.2. Iani Chaos

[12] Iani Chaos (Figure 6) is roughly 400 km in diameter and is centered at 342.3°E, 2.0°S. It is the primary source region of Ares Vallis, an outflow channel that extends to the northwest and terminates in Chryse Planitia. Like Aureum Chaos, it is characterized by jumbled chaotic terrain, layered light-toned deposits (Figure 6b), and a hematite-rich unit. The light-toned units have a TES albedo of ∼0.17–0.19 compared to an albedo of ∼.13–.15 for the surrounding chaotic terrain. In addition, the nighttime temperatures of
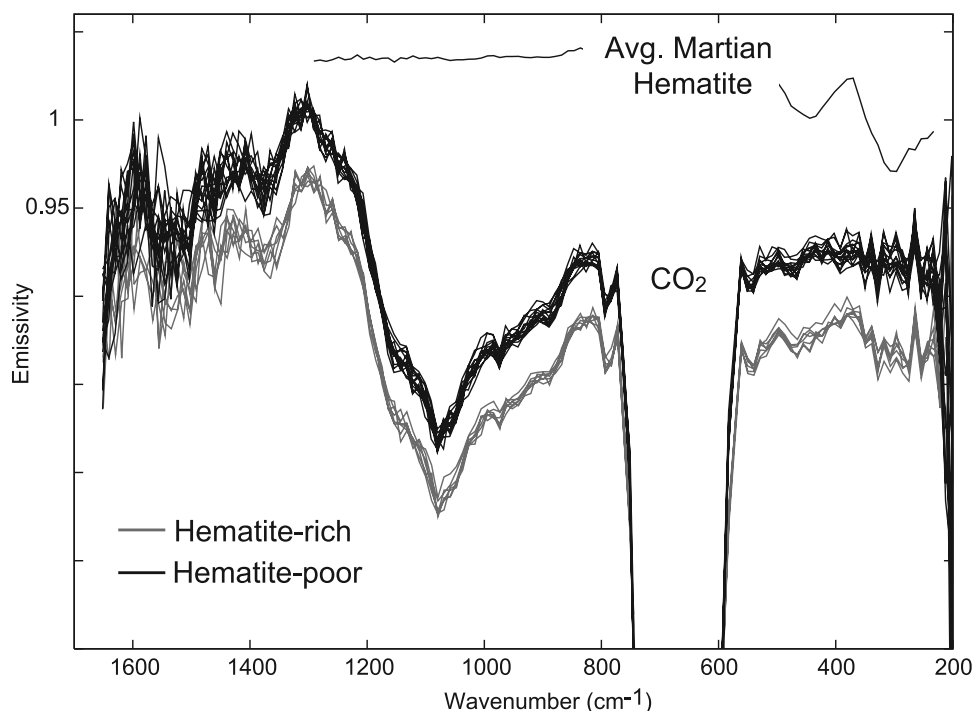
Figure 5. TES spectra (OCK 3475, ICKs 1703-1706) over Aureum Chaos. The hematite spectral features in the red spectra are easily observed at ~300 and 540 cm^{-1}. Spectra are offset for clarity.

the light-toned units are generally warmer than the surrounding terrain (Figure 3b), indicating either increased rock abundance or an increased level of cementation. The TES thermal inertia of the light-toned units ranges from $\sim320-360$ Jm^{-2} s$^{-1/2}$ K^{-1} compared to range of $\sim260-300$ for the surrounding chaotic terrain. In Iani Chaos, cliff-forming light-toned units are not as common as those observed in Aureum and Iani Chaos. While cliff-forming deposits are observed, in most cases the light-toned units appear to be finely layered and interbedded with darker layered deposits. Another difference between Iani Chaos and Aureum and Aram Chaos is that the hematite-rich unit observed in Iani Chaos appears to be coincident with the light-toned deposits rather than stratigraphically below them. The light-toned units appear to be interbedded with darker layered units (Figure 7a), and as in Aureum Chaos, "tentative light-toned units" are also observed within some chaotic mounds (Figure 7b). However, MOC NA imagery also reveals cases in which light-toned deposits on-lap chaotic mounds (Figures 7c and 7d). Hematite abundance varies between $5-20\%$, although the majority of the unit exhibits an abundance of $5-10\%$ which is less than is seen in other hematite-rich units on Mars. The highest hematite abundance (Figure 6b) is associated with a layered unit that is slightly darker than the surrounding lighter-toned material (TES albedo of ~0.16 compared to $\sim0.17-0.19$).

3.3. Composition of the Light-Toned Units

[13] As discussed, the light-toned units in Aureum and Iani Chaos have been reported to be sulfate-rich on the basis of data returned from the OMEGA visible/near-IR spectrometer [Gendrin et al., 2005; Noe Dobrea et al., 2006a; Noe Dobrea, 2006]. Using THEMIS VIS color imagery of these deposits, we can also semi-quantitatively assess their

ferric iron content. The light-toned units in Aram, Aureum and Iani Chaos, including "tentative" light-toned exposures (section 3.1), display a deeper 540 nm band depth than the surrounding terrain (Figure 8). The case of Iani Chaos is less clear, although some difference between the light-toned units and the surrounding terrain is evident.

[14] The increased redness seen in the Aram, Aureum and Iani light-toned units is likely due to an increased abundance of ferric iron relative to the surrounding basalt-dominated terrains. While increased redness could be attributable to surface dust, it is unlikely that dust would preferentially deposit on the light-toned units. In addition, in Aram Chaos, the cap unit is discontinuously covered by dark sand [Glotch and Christensen, 2005], supporting the unlikelihood of dust preservation on the surface. Finally, the 540 nm feature has been shown to be diagnostic of crystalline red hematite [Bell et al., 1990, 2004; Bishop et al., 1998; Morris et al., 2000; Bell et al., submitted manuscript, 2006] rather than nanophase iron oxides which are thought to be the red pigment in the globally homogenous Martian dust [Morris et al., 1989; Morris and Lauer, 1990].

4. Discussion

4.1. Evaluation of Formation Models for the Hematite and Light-Toned Units in Chaotic Terrains

[15] Formation hypotheses put forth for the hematite-bearing, sulfate-rich outcrop in Meridiani Planum include subaqueous/groundwater [Christensen and Ruff, 2004; Squyres et al., 2004; Squyres and Knoll, 2005; Grotzinger et al., 2005; McLennan et al., 2005] depositional mechanisms, volcanic [McCollom and Hynek, 2005], and impact-related [Knauth et al., 2005] mechanisms. Chaotic terrains
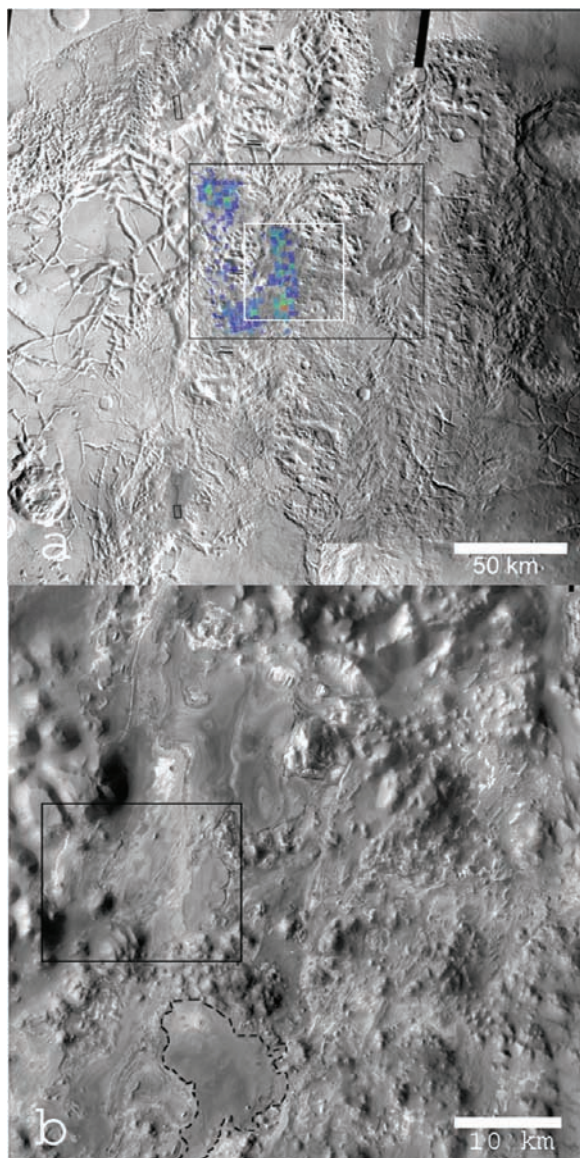
Figure 6. Hematite and light-toned deposits in Iani Chaos. (a) TES hematite abundance overlaid on THEMIS daytime IR radiance mosaic. Hematite abundance ranges from 5% (blue) to 20% (red). The white outline shows the location of Figure 6b. The large black outline shows the location of Figure 3b. The small black outline at the bottom left shows the location of Figure 7b. The small black outline at the top left shows the location of Figures 7c and 7d. (b) THEMIS visible band 3 mosaic consisting of images V10961001, V18324001, V16789001, V10649001, V18012002, V16477001, V01774001, V14942001, V10025001, V06243001, V13095001, V16165001, V12783001, V14318001, V17388001, V08465001, V14006001, and V08802001, showing the light-toned, layered unit in the area of highest hematite concentration (dashed line). Similar layered units to the west and north have slightly lower hematite concentrations. Sulfates were detected in this region using OMEGA data [*Gendrin et al.*, 2005]. The solid black outline shows the location of Figure 7a.

are widely thought to have formed when the release of subsurface material caused fracture and slumping of the surface. Because of the close proximity of many chaotic terrains to large outflow channels, the preferred formation mechanism involves the breakthrough of groundwater to the surface [*Sharp*, 1973], either due to the melting of a permafrost layer by a volcanic intrusion [*Maxwell and Picard*, 1974; *Masursky et al.*, 1977], the release of a high-pressure confined aquifer beneath a permafrost layer [*Carr*, 1979], the dissolution of subsurface clathrate hydrates [*Komatsu et al.*, 2000; *Max and Clifford*, 2000], or the catastrophic dewatering of subsurface hydrous sulfates which may have been heated by Hesperian-aged lava flows *Montgomery and Gillespie* [2005]. Others have suggested a volcanic eruptive origin for the formation of at least some chaotic terrains [*Chapman and Tanaka*, 2002]. Release of the subsurface material and the formation of the outflow channels have been thought to form in catastrophic events [*Baker et al.*, 1992], but both numerical modeling [*Hanna and Phillips*, 2003; *Harrison and Grimm*, 2007] and geomorphologic evidence [*Rodriguez et al.*, 2005] suggest that release of subsurface water likely occurred over several episodes and was not necessarily a catastrophic event in each case. The non-catastrophic release of subsurface water increases the likelihood of water having ponded in the chaotic terrains, even if it was for a geologically short period of time.

[16] The hematite and sulfate-bearing deposits shown in this work lie only within the chaotic terrains and are absent on the surrounding plains. It is unlikely that volcanic or impact processes would preferentially leave deposits within the chaotic terrains but not on the surrounding plains, although it is possible that aeolian processes may have been more effective at eroding light-toned deposits on the plains than in the basins in which they are currently seen. Furthermore, the spectral nature of the hematite as determined by TES is inconsistent with the formation of hematite in a high-temperature environment [*Glotch et al.*, 2004], as would be required by these models. In addition, *Catling et al.* [2006] calculate that gypsum ($CaSO_4 \bullet 2H_2O$), which is the best fit for sulfates detected in Iani Chaos [*Gendrin et al.*, 2005], will only be produced in depositional settings less than ~60°C. At higher temperatures, anhydrite ($CaSO_4$), rather than gypsum is produced. It is possible, however, that anhydrite could have been produced in a high-temperature setting, and later hydrated to gypsum if the system cooled and water remained persistent. On the basis of (1) geologic evidence that chaos formation likely involved water, (2) the lack of capping, hematite, or sulfate-rich units on the surrounding plains, and (3) spectral and geochemical evidence for low-temperature aqueous processes, we conclude that the hematite and cap units found in chaotic terrains likely formed in an aqueous environment.

4.2. Comparison to Meridiani Planum Units

[17] The properties of the crystalline hematite and light-toned units in Aureum and Iani Chaos determined from orbital observations are similar to those of the bedrock and hematite observed at Meridiani Planum. At the MER Opportunity site in Eagle crater, hematite was detected in spherules as well as in the outcrop matrix [*Klingelhöfer et al.*, 2004; *Christensen et al.*, 2004a; *Morris et al.*, 2006].
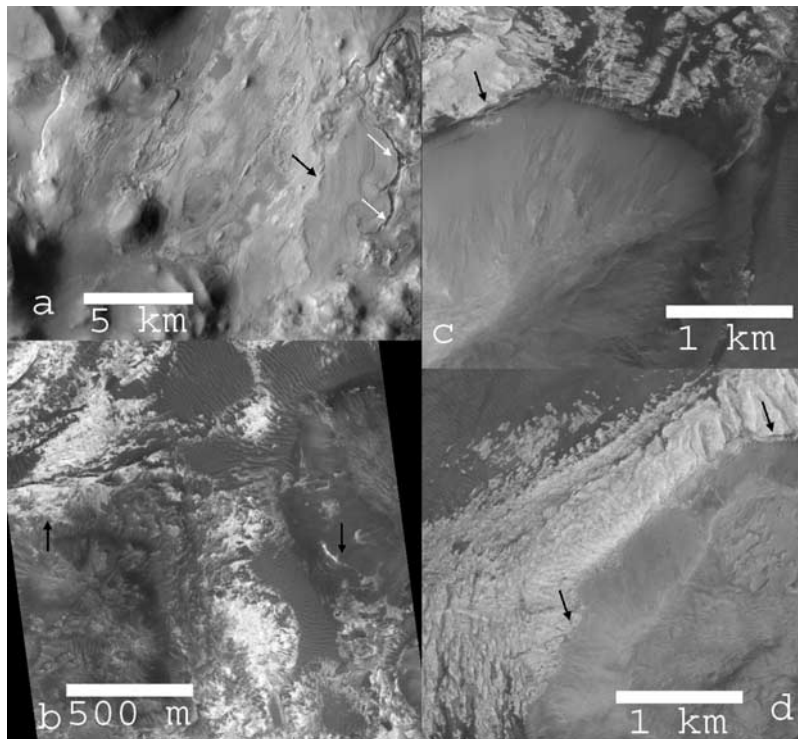
Figure 7. Light-toned materials in Iani Chaos are present both above and within chaotic terrain. (a) THEMIS VIS band 3 mosaic consisting of images V01774001 and V16789001. Light-toned material overlays intermediate-toned layered deposits (black arrow). White arrows show intermediate-toned layered deposits overlaying chaotic units. (b) Portion of MOC NA image R10-01264. Arrows point to light-toned material that is exposed on top of and within chaotic mounds. (c) Portion of MOC NA R15-00919 showing light-toned material on-lapping a small knob (arrow). (d) Portion of same MOC image showing light-toned material on-lapping another knob (arrows).

The Eagle crater outcrop has an average Fe^{3+}/Fe_{total} of 0.88 as opposed to an average Fe^{3+}/Fe_{total} of 0.37 for basaltic soils [*Klingelhöfer et al.*, 2004], indicating the presence of crystalline hematite. Furthermore, Mössbauer analyses show a high Fe content in spherule-free outcrop targets, indicating that the hematite is dispersed throughout the outcrop matrix as well as in the spherules. THEMIS VIS data from light-toned units in chaotic terrain are consistent with the presence of red crystalline hematite (Figure 8). This similarity may imply a common formation mechanism for these light-toned units. The light-toned units observed at Meridiani Planum have also been shown to be sulfate-rich [*Squyres et al.*, 2004; *McLennan et al.*, 2005], and MiniTES data indicate the presence of both Ca- and Mg-rich sulfates [*Christensen et al.*, 2004a; *Glotch et al.*, 2006]. Sulfate enrichments have been identified in the chaos terrains in OMEGA data [*Gendrin et al.*, 2005; *Noe Dobrea et al.*, 2006a; *Noe Dobrea*, 2006], including the presence of gypsum in Iani Chaos. Finally, TES data indicate similar concentrations of gray crystalline hematite in Meridiani Planum and the chaos terrains, with abundances ranging between 5–20% in both areas. The shared characteristics between the chaos units and the outcrops at Meridiani Planum suggest a similar formation mechanism. If the chaos units are aqueous in origin (as discussed in section 4.1), then the presence of hematite and sulfate-bearing units that are similar to Meridiani Planum in Aureum, Iani, and Aram

Chaos is problematic for models that invoke an impact base surge [*Knauth et al.*, 2005] or volcanic [*McCollom and Hynek*, 2005] origin for deposition of sulfate-rich bedrock and hematite mineralization in Meridiani Planum.

[18] Finally, we note that Aram, Aureum, and Iani Chaos share similar stratigraphic sequences, in that light-toned and hematite-rich units are superposed on chaotically disturbed units, and that Meridiani Planum may also share these characteristics. Polygonal features in eastern Meridiani Planum (Figure 9) previously interpreted as volcanic in origin [*Arvidson et al.*, 2003] resemble polygonal fracturing seen in the chaotic terrains. It is possible that these positive-relief features, which lie stratigraphically below the light-toned "etched" unit and the hematite-bearing unit [*Arvidson et al.*, 2003; *Edgett*, 2005] could be the remnants of a resistant "paleochaos" fracture fill in Meridiani Planum.

4.3. Proposed Sequence of Events in Aureum and Iani Chaos

[19] Aureum and Iani Chaos have likely undergone a complex set of geological processes leading to their present-day status. Light-toned, reddish, sulfate-rich cap units superpose chaotic blocks in both Aureum and Iani Chaos (section 3). In addition, there is evidence for light-toned material within and below chaotic mounds, although the similarity to cap units is uncertain (sections 3.1 and 3.2). Below we outline two possible sequences of events for the
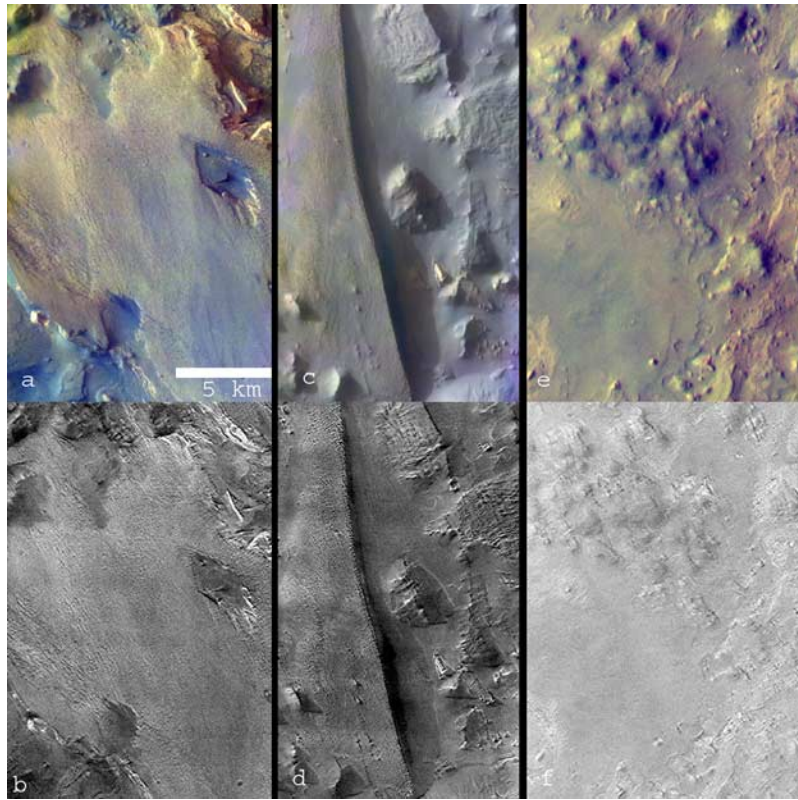
Figure 8. THEMIS VIS false color images composed from visible bands 3, 2, and 1 and THEMIS VIS 540 nm band depth images derived using the method described in section 2. In the band depth images, the light-toned deposits are brighter than the surrounding terrain, indicating increased ferric iron content. The same stretch has been applied to all three images. In the corresponding false color images, the light-toned deposits appear redder than the surrounding terrain. All images are at the same scale. (a) Aram Chaos bands 3, 2, and 1 false color image created from a portion of THEMIS VIS image V05618015. (b) Aram Chaos 540 nm band depth image created from a portion of THEMIS VIS image V05618015. (c) Aureum Chaos bands 3, 2, and 1 false color image created from a portion of THEMIS VIS image V11760001. (d) Aureum Chaos 540 nm band depth image created from a portion of THEMIS VIS image V11760001. (e) Iani Chaos bands 3, 2, and 1 false color image created from a portion of THEMIS VIS image V10025001. (f) Iani Chaos 540 nm band depth image created from a portion of THEMIS VIS image V10025001.

formation of the chaos units; the scenarios differ only slightly based on whether the light-toned material observed within the chaotic blocks is interpreted as (1) a cap-like sulfate-rich unit or (2) a unit that is unlike cap materials (such as typical basaltic crust). Our proposed sequence of events is based on analogy to the MER team model for outcrop and spherule formation in Meridiani Planum.

[20] In the first scenario, the regions where Aureum and Iani Chaos presently stand were once playa-like environments similar to that suggested for Meridiani Planum in the Noachian [*Squyres and Knoll*, 2005]. Light-toned rocks, which we now see as small exposures within and below the chaotic mounds were deposited in a shallow water or groundwater-rich environment. There is no constraint on the earliest time at which these light-toned exposures could have formed, but timing similar to the formation of similar units in Meridiani Planum (Noachian) is reasonable. Following deposition of the light-toned deposits, the release of subsurface water produced the chaos terrain during the mid to late Hesperian [*Rotto and Tanaka*, 1995; *Tanaka et al.*, 2003]. Following the formation of the chaotic blocks and knobby terrains, several episodes of groundwater recharge and release [*Hanna and Phillips*, 2003; *Rodriguez et al.*, 2005] facilitated ponding and deposition of the capping light-toned unit. Aeolian reworking of the cap unit may or may not have occurred; from orbit it is difficult to tell if the light-toned outcrops in chaotic terrains are truly evaporites or reworked evaporitic standstones. During the later episodes of groundwater recharge and flow, hematite may have been formed by secondary diagenetic processes, similar to the MER team's model for hematite formation in Meridiani Planum [*Squyres and Knoll*, 2005; *McLennan et al.*, 2005]. Subsequent to the lithification of these units, aeolian activity stripped away much of the light-toned material leading to the present-day configuration. The MER Opportunity Rover revealed that the detection of hematite by TES from orbit was facilitated by the presence of hematite in a concentrated lag deposit on the Meridiani Plains. The infrared spectral signature of hematite spherules, though present in the outcrop, is difficult to detect in MiniTES spectra because
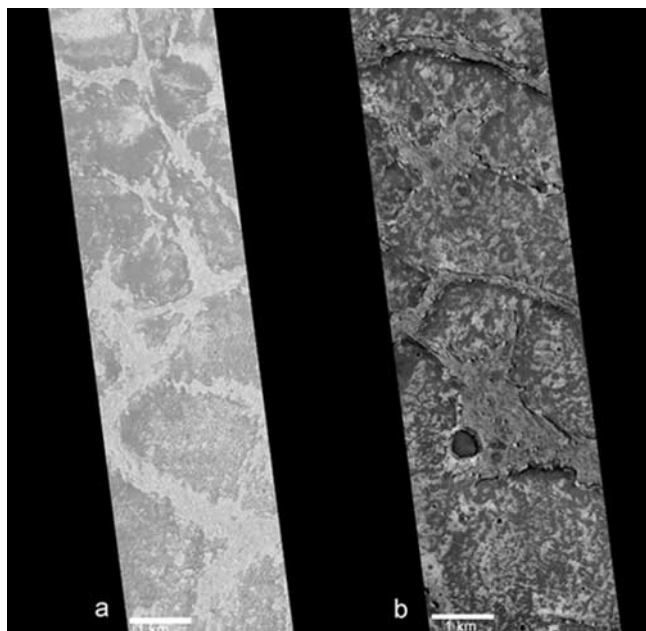
Figure 9. Two examples of possible "paleochaos" in eastern Meridiani Planum, which lies stratigraphically below light-toned "etched" terrain and hematite-bearing layered unit [*Arvidson et al.*, 2003; *Edgett*, 2005]. (a) MOC NA 1201466. (b) MOC NA M0401901.

their areal concentration is less than ~5% [*Christensen et al.*, 2004a; *Glotch et al.*, 2006]. We suggest that hematite in Valles Marineris, Aram, Aureum, and Iani Chaos may be present in the same form as is seen at Meridiani Planum. If that is so, then the hematite signatures detected in these regions from orbit are also likely to be concentrated lag deposits.

[21] In the second scenario, the playa or lacustrine-like conditions did not begin until after the formation of the chaos terrain (mid to late Hesperian). The cap unit formed under these conditions and repeated groundwater recharge facilitated hematite formation. The hematite was later concentrated as a lag through erosion of the cap units.

4.4. Global View of Gray, Crystalline Hematite

[22] Here we explore ways in which units in Meridiani Planum and the chaos terrains may or may not be related in timing and origin. The sulfate-rich unit in Meridiani Planum is Noachian in age [*Hynek et al.*, 2002; *Lane et al.*, 2003]. Chaos cap units are late Hesperian in age [*Rotto and Tanaka*, 1995; *Tanaka et al.*, 2003]. These observations indicate that conditions for forming sulfate-rich terrains in the Meridiani Planum region of Mars ceased during the Noachian time period, but continued through the Hersperian in chaos regions. It is not clear if sulfate-rich deposits began forming before or after the chaos formed (section 4.3). However, it must be that either the formation of sulfates in Meridiani Planum and the chaos terrains started at different times, or that sulfate formation in the chaos terrains started around the same time as in Meridiani Planum, but then persisted for much longer.

[23] Hematite in the chaotic terrains, if formed diagenetically within the light-toned units, must be late Hesperian in age or younger. As already stated, in Meridiani Planum, the light-toned outcrop was deposited during the Noachian [*Hynek et al.*, 2002; *Lane et al.*, 2003], but there is no constraint on when hematite diagenesis occurred. Thus it is possible that gray crystalline hematite in Meridiani Planum and the chaos terrains formed at the same time (late Hesperian or younger) and may indicate a large regional process/event.

[24] Finally, it is possible that polygonal fractures observed in Meridiani Planum are remnants of chaos-like features (section 4.2). Is so, this would imply that the chaos formation in this region occurred much earlier (by ~1 Gyr) than the Hesperian-aged chaos terrains to the west.

5. Conclusions

[25] Gray crystalline hematite deposits associated with light-toned, sulfate-rich units are present in Aureum and Iani Chaos. The hematite-rich units lie stratigraphically above chaotic mounds, indicating that they were deposited subsequent to the formation of the chaotic terrains. Light-toned units occur stratigraphically above, and sometimes within, chaotic mounds, potentially suggesting several episodes of formation which bracket the formation of the chaotic terrains.

[26] The light-toned units have been described as sulfate-rich [*Gendrin et al.*, 2005; *Noe Dobrea et al.*, 2006a; *Noe Dobrea*, 2006], and on the basis of multispectral THEMIS VIS images, they may also contain red crystalline hematite. The association of light-toned sulfate-rich deposits with red crystalline hematite and their close proximity to the gray crystalline hematite deposits detected by TES suggests a similar formation mechanism to the light-toned outcrop and hematite lag seen by the MER Opportunity rover at Meridiani Planum. Moreover, neither light-toned nor hematite-rich deposits are detected outside of the chaotic terrains in the mapped region (Figure 1), suggesting that volcanic or impact mechanisms [*McCollom and Hynek*, 2005; *Knauth et al.*, 2005] for the formation of these units is unlikely.

[27] We propose a shallow water or groundwater depositional environment for the formation of the light-toned and hematite-rich units in Aureum and Iani Chaos. The light-toned deposits in Aram, Aureum and Iani Chaos were deposited following the release of subsurface water and the formation of the chaotic terrains. Reactivation of the groundwater source could have provided the necessary diagenetic conditions for the formation of secondary hematite. If the initial chaos formation was caused by the melting and eruption of subsurface ice by a regional heat source, then this heat source may have also been responsible for the continued reactivation of groundwater and the diagenetic formation of hematite. Exposures of light-toned material seen within the chaotic mounds in these regions may be analogous in composition to the cap units and could have formed coevally with the Noachian light-toned outcrop observed at Meridiani Planum. However, the light-toned and gray hematite-rich deposits that lie stratigraphically above the chaotic terrain must have formed much later, in the mid to late Hesperian. Hematite-rich spherules in Meridiani Planum might have also formed this late, implying the continued presence of groundwater long after the formation of the sulfate-rich sedimentary rocks.

References

Arvidson, R. E., F. P. Seelos IV, K. S. Deal, W. C. Koeppen, N. O. Snider, J. M. Kieniewicz, B. M. Hynek, M. T. Mellon, and J. B. Garvin (2003), Mantled and exhumed terrains in Terra Meridiani, Mars, *J. Geophys. Res.*, *108*(E12), 8073, doi:10.1029/2002JE001982.

Baker, V. R., H. C. Carr, V. C. Gulick, C. R. Williams, and M. S. Marley (1992), Channels and valley networks, in *Mars*, edited by H. H. Kieffer et al., pp. 493–522, Univ. of Ariz. Press, Tucson.

Bandfield, J. L., P. R. Christensen, and M. D. Smith (2000), Spectral data set factor analysis and end-member recovery: Application to analysis of Martian atmospheric particulates, *J. Geophys. Res.*, *105*(E4), 9573–9587.

Bandfield, J. L., K. S. Edgett, and P. R. Christensen (2002), Spectroscopic study of the Moses Lake dune field, Washington: Determination of compositional distributions and source lithologies, *J. Geophys. Res.*, *107*(E11), 5092, doi:10.1029/2000JE001469.

Bell, J. F., III, T. B. McCord, and P. D. Owensby (1990), Observational evidence of crystalline iron oxides on Mars, *J. Geophys. Res.*, *95*(B9), 14,447–14,461.

Bell, J. F., III, et al. (2004), Pancam multispectral imaging results from the Opportunity Rover at Meridiani Planum, *Science*, *306*, 1703–1709.

Bibring, J.-P., et al. (2005), Mars surface diversity as revealed by the OMEGA/Mars Express observations, *Science*, *307*, 1576–1581.

Bishop, J. L., H. Fröschl, and R. Mancinelli (1998), Alteration processes in volcanic soils and identification of exobiologically important weathering products on Mars using remote sensing, *J. Geophys. Res.*, *103*(E13), 31,457–31,476.

Carr, M. H. (1979), Formation of Martian flood features by release of water from confined aquifers, *J. Geophys. Res.*, *84*, 2995–3007.

Catling, D. C., and J. M. Moore (2003), The nature of coarse-grained crystalline hematite and its implications for the early environment of Mars, *Icarus*, *165*, 277–300.

Catling, D. C., S. E. Wood, C. Leovy, D. R. Montgomery, H. M. Greenberg, C. R. Glein, and J. M. Moore (2006), Light-toned layered deposits in Juventae Chasma, Mars, *Icarus*, *181*, 26–51.

Chapman, M. G., and K. L. Tanaka (2002), Related magma-ice interactions: Possible origins of chasmata, chaos, and surface materials in Xanthe, Margaritifer, and Meridiani Terrae, Mars, *Icarus*, *155*, 324–339.

Christensen, P. R., and S. W. Ruff (2004), Formation of the hematite-bearing unit in Meridiani Planum: Evidence for deposition in standing water, *J. Geophys. Res.*, *109*, E08003, doi:10.1029/2003JE002233.

Christensen, P. R., et al. (2000), Detection of crystalline hematite mineralization on Mars by the Thermal Emission Spectrometer: Evidence for near-surface water, *J. Geophys. Res.*, *105*, 9623–9642.

Christensen, P. R., R. V. Morris, M. D. Lane, J. L. Bandfield, and M. C. Malin (2001), Global mapping of Martian hematite deposits: Remnants of water-driven processes on early Mars, *J. Geophys. Res.*, *106*, 23,873–23,886.

Christensen, P. R., et al. (2004a), Mineralogy at Meridiani Planum from the Mini-TES experiment on the Opportunity rover, *Science*, *306*, 1733–1739.

Christensen, P. R., et al. (2004b), The Thermal Emission Imaging System (THEMIS) for the Mars 2001 Odyssey mission, *Space. Sci. Rev.*, *110*, 85–130.

Edgett, K. S. (2005), The sedimentary rocks of Sinus Meridiani: Five key observations from data acquired by the Mars Global Surveyor and Mars Odyssey orbiters, *Mars*, *1*, 5–58, doi:10.1555/mars/2005.0002.

Gendrin, A., et al. (2005), Sulfates in Martian layered terrains: The OMEGA/Mars Express view, *Science*, *307*, 1587–1590.

Glotch, T. D., and P. R. Christensen (2005), Geologic and mineralogic mapping of Aram Chaos: Evidence for a water-rich history, *J. Geophys. Res.*, *110*, E09006, doi:10.1029/2004JE002389.

Glotch, T. D., R. V. Morris, P. R. Christensen, and T. G. Sharp (2004), Effect of precursor mineralogy on the thermal infrared emission spectra of hematite: Application to Martian hematite mineralization, *J. Geophys. Res.*, *109*, E07003, doi:10.1029/2003JE002224.

Glotch, T. D., J. L. Bandfield, P. R. Christensen, W. M. Calvin, S. M. McLennan, B. C. Clark, A. D. Rogers, and S. W. Squyres (2006), Mineralogy of the light-toned outcrop at Meridiani Planum as seen by the Miniature Thermal Emission Spectrometer and implications for its formation, *J. Geophys. Res.*, *111*, E12S03, doi:10.1029/2005JE002672.

Gorelick, N. S., M. Weiss-Malik, B. Steinberg, and S. Anwar (2003), JMARS: A multimission data fusion application, *Lunar Planet. Sci.* [CD-ROM], *XXXIV*, abstract 2057.

Grotzinger, J. P., et al. (2005), Stratigraphy and sedimentology of a dry to wet eolian depositional system, Burns formation, Meridiani Planum, Mars, *Earth Planet. Sci. Lett.*, *240*, 11–72.

Hanna, J. C., and R. J. Phillips (2003), Theoretical modeling of outflow channels and chaos regions on Mars, *Eos Trans. AGU*, *84*(46), Fall Meet. Suppl., Abstract P11B-1036.

Harrison, K. P., and R. E. Grimm (2007), Multiple flooding events in Martian outflow channels: Quantitative considerations, *Lunar Planet. Sci.* [CD-ROM], *XXXVIII*, abstract 1375.

Herkenhoff, K. E., et al. (2004), Evidence from Opportunity's Microscopic Imager for water on Meridiani Planum, *Science*, *306*, 1727–1730.

Hynek, B. M., R. E. Arvidson, and R. J. Phillips (2002), Geologic setting and origin of Terra Meridiani hematite deposit on Mars, *J. Geophys. Res.*, *107*(E10), 5088, doi:10.1029/2002JE001891.

Jakosky, B. M., M. T. Mellon, H. H. Kieffer, P. R. Christensen, E. S. Varnes, and S. W. Lee (2000), The thermal inertia of Mars from the Mars Global Surveyor Thermal Emission Spectrometer, *J. Geophys. Res.*, *105*, 9643–9652.

Klingelhöfer, G., et al. (2004), Jarosite and hematite at Meridiani Planum from Opportunity's Mössbauer Spectrometer, *Science*, *306*, 1740–1745.

Knauth, L. P., D. M. Burt, and K. H. Wohletz (2005), Impact origin of sediments at the Opportunity landing site on Mars, *Nature*, *438*, 1123–1128.

Knudson, A. T. (2006), Dirty rocks: Thermal infrared studies of dusty, sandy, or coated soils and rocks on Mars and Earth, Ph.D. dissertation, Ariz. State Univ., Tempe.

Komatsu, G., J. S. Kargel, V. R. Baker, R. G. Strom, G. G. Ori, C. Mosangini, and K. L. Tanaka (2000), A chaotic terrain formation hypothesis: Explosive outgas and outflow by dissociation of clathrate on Mars, *Lunar Planet. Sci.* [CD-ROM], *XXXI*, abstract 1434.

Lane, M. D., P. R. Christensen, and W. K. Hartmann (2003), Utilization of the THEMIS visible and infrared imaging data for crater population studies of the Meridiani Planum landing site, *Geophys. Res. Lett.*, *30*(14), 1770, doi:10.1029/2003GL017183.

Malin, M. C., G. E. Danielson, M. A. Ravine, and T. A. Soulanille (1991), Design and development of the Mars Observer Camera, *Int. J. Imaging Syst. Technol.*, *3*, 76–91.

Malin, M. C., G. E. Danielson, A. P. Ingersoll, H. Masursky, J. Veverka, M. A. Ravine, and T. A. Soulanille (1992), Mars Observer Camera, *J. Geophys. Res.*, *97*, 7699–7718.

Malinowski, E. R. (1991), *Factor Analysis in Chemistry*, 2nd ed., John Wiley, Hoboken, N. J.

Masursky, H., J. M. Boyce, A. L. Dial, G. G. Schaber, and M. E. Strobell (1977), Classification and time of formation of Martian channels based on Viking data, *J. Geophys. Res.*, *82*, 4016–4038.

Max, M. D., and S. M. Clifford (2000), The initiation of Martian outflow channels through the catastrophic decomposition of methane hydrate, *Lunar Planet. Sci.* [CD-ROM], *XXXI*, abstract 2094.

Maxwell, T. A., and M. D. Picard (1974), Evidence of subsurface water in equatorial regions of Mars, *AAPG Bull.*, *58*, 915.

McCollom, T. M., and B. M. Hynek (2005), A volcanic environment for bedrock diagenesis at Meridiani Planum on Mars, *Nature*, *438*, 1129–1131.

McConnochie, T. H., and J. F. Bell III (2003), Visible imager calibration, in *2001 Mars Odyssey Thermal Emission Imaging System Data Processing User's Guide*, edited by P. R. Christensen et al., pp. 21–37, NASA Planet. Data Syst., Pasadena, Calif. (Available at http://pdsimg.jpl.nasa.gov/Atlas/DocLinks.html#2001_MARS_ODYSSEY)

McConnochie, T. H., J. F. Bell III, D. Savransky, G. Mehall, M. Caplinger, P. R. Christensen, L. Cherednik, K. Bender, and A. Dombovari (2006), Calibration and in-flight performance of the Mars Odyssey Thermal Emission Imaging System visible imaging subsystem (THEMIS VIS), *J. Geophys. Res.*, *111*, E06018, doi:10.1029/2005JE002568.

McLennan, S. M., et al. (2005), Provenance and diagenesis of the evaporite-bearing Burns formation, Meridiani Planum, Mars, *Earth Planet. Sci. Lett.*, *240*, 95–121.

Mellon, M. T., B. M. Jakosky, H. H. Kieffer, and P. R. Christensen (2000), High-resolution thermal inertia mapping from the Mars Global Surveyor Thermal Emission Spectrometer, *Icarus*, *148*, 437–455.

Montgomery, D. R., and A. Gillespie (2005), Formation of Martian outflow channels by catastrophic dewatering of evaporite deposits, *Geology*, *33*, 625–628.

Morris, R. V., and H. V. Lauer Jr. (1990), Matrix effects for reflectivity spectra of dispersed nanophase (superparamagnetic) hematite with application to Martian spectral data, *J. Geophys. Res.*, 95, 5101–5109.

Morris, R. V., D. G. Argresti, H. V. Lauer Jr., J. A. Newcomb, T. D. Shelfer, and A. V. Murali (1989), Evidence for pigmentary hematite on Mars based on optical, magnetic, and Mössbauer studies of superparamagnetic (nanocrystalline) hematite, *J. Geophys. Res.*, 94, 2760–2778.

Morris, R. V., et al. (2000), Mineralogy, composition, and alteration of Mars Pathfinder rocks and soils: Evidence from multispectral, elemental, and magnetic data on terrestrial analogue, SNC meteorite, and Pathfinder samples, *J. Geophys. Res.*, 105(E1), 1757–1817.

Morris, R. V., et al. (2006), Mössbauer mineralogy of rock, soil, and dust at Meridiani Planum, Mars: Opportunity's journey across sulfate-rich outcrop, basaltic sand and dust, and hematite lag deposits, *J. Geophys. Res.*, 111, E12S15, doi:10.1029/2006JE002791.

Noe Dobrea, E. Z. (2006), Correlation between sulfate and hematite deposits as observed by OMEGA and TES, paper presented at Workshop on Martian Sulfates as Recorded by Atmospheric-Fluid-Rock Interactions, Lunar and Planet. Inst., Houston, Tex.

Noe Dobrea, E. Z., F. Poulet, and M. C. Malin (2006a), Omega analysis of light toned outcrops in the chaotic terrain of the eastern Valles Marineris region, *Lunar Planet. Sci.* [CD-ROM], XXXVII, abstract. 2068.

Noe Dobrea, E. Z., J. F. Bell III, T. H. McConnochie, and M. Malin (2006b), Analysis of a spectrally unique deposit in the dissected Noachian terrain of Mars, *J. Geophys. Res.*, 111, E06007, doi:10.1029/2005JE002431.

Poulet, F., J.-P. Bibring, J. F. Mustard, A. Gendrin, N. Mangold, Y. Langevin, R. E. Arvidson, B. Gondet, and C. Gomez (2005), Phyllosilicates on Mars and implications for early Martian climate, *Nature*, 438, 623–627.

Presley, M. A., and P. R. Christensen (1997), Thermal conductivity measurements of particulate materials: 2. Results, *J. Geophys. Res.*, 102, 6551–6556.

Ramsey, M. S., and P. R. Christensen (1998), Mineral abundance determination: Quantitative deconvolution of thermal emission spectra, *J. Geophys. Res.*, 103, 577–596.

Rieder, R., et al. (2004), Chemistry of rocks and soils at Meridiani Planum from the Alpha Particle X-ray Spectrometer, *Science*, 306, 1746–1749.

Rodriguez, J. A. P., S. Sasaki, R. O. Kuzmin, J. M. Dohm, K. L. Tanaka, H. Miyamoto, K. Kurita, G. Komatsu, A. G. Fairén, and J. C. Ferris (2005), Outflow channel sources, reactivation, and chaos formation, Xanthe Terra, Mars, *Icarus*, 175, 36–57.

Rotto, S., and K. L. Tanaka (1995), Geologic/geomorphic map of the Chryse Planitia region of Mars, *U.S. Geol. Surv. Misc. Invest. Ser.*, Map I-2441.

Sharp, R. P. (1973), Mars: Fretted and chaotic terrains, *J. Geophys. Res.*, 78, 4073–4083.

Smith, D. E., et al. (2001), Mars Orbiter Laser Altimeter: Experiment summary after the first year of global mapping of Mars, *J. Geophys. Res.*, 106, 23,689–23,722.

Soderblom, L. A., et al. (2004), Soils of Eagle Crater and Meridiani Planum at the Opportunity Rover landing site, *Science*, 306, 1723–1726.

Squyres, S. W., and A. H. Knoll (2005), Sedimentary rocks at Meridiani Planum: Origin, diagenesis, and implications for life on Mars, *Earth Planet. Sci. Lett.*, 240, 1–10.

Squyres, S. W., et al. (2004), In situ evidence for an ancient aqueous environment at Meridiani Planum, Mars, *Science*, 306, 1709–1714.

Squyres, S. W., et al. (2006), Overview of the Opportunity Mars Exploration Rover Mission to Meridiani Planum: Eagle Crater to Purgatory Ripple, *J. Geophys. Res.*, 111, E12S12, doi:10.1029/2006JE002771.

Tanaka, K. L., J. A. Skinner Jr., T. M. Hare, T. Joyal, and A. Wenker (2003), Resurfacing history of the northern plains of Mars based on geologic mapping of Mars Global Surveyor data, *J. Geophys. Res.*, 108(E4), 8043, doi:10.1029/2002JE001908.

Zuber, M. T., D. E. Smith, S. C. Solomon, D. O. Muhleman, J. W. Head, J. B. Garvin, J. B. Abshire, and J. L. Bufton (1992), The Mars Observer Laser Altimeter investigation, *J. Geophys. Res.*, 97, 7781–7797.

————————————

T. D. Glotch, Division of Geological and Planetary Sciences, California Institute of Technology, MC 150-21, Pasadena, CA 91125, USA. (tglotch@gps.caltech.edu)

A. D. Rogers, Division of Geological and Planetary Sciences, California Institute of Technology, Pasadena, CA 91125, USA.